Indonesian Journal of Electrical Engineering and Computer Science
Vol. 1, No. 3, March 2016, pp. 464 ~ 479
DOI: 10.11591/ijeecs.v1.i3.pp464-479

Distance Relay Impedance Measuring Problems in Presence of Wind Farms

Farhad Namdari*, Fatemeh Soleimani, Esmaeel Rokrok
Department of Electrical Engineering, Lorestan Universiy,
Khorramabad, Lorestan, Iran
*e-mail: Namdari.f@lu.ac.ir

Abstract

Environmental concerns along with the increasing demand on electrical power, have led to power generation of renewable sources like wind. Connecting wind turbines in large scale powers with transmission network makes new challenges like the impact of these renewable sources on power system protection. This paper studies the impact of fault resistance and its location on voltage and current fundamental frequencies of faulted lines connected to DFIG based wind farms and it will be demonstrated that because of the large differences between these frequencies, impedance measuring of distance relays is inefficient. Hence in these power systems using conventional impedance measurements is not suitable anymore and new impedance measuring approaches are required in distance relays.

Keywords*: Transmission line, DFIG-based wind farm, impedance measurement*

1. Introduction

Increasing demand on electrical power, fossil fuel power plants environmental issues, and high cost of electricity have led to global trend inclean and free renewable sources of energy like wind. Electricity generationof wind energy in large-scales is more economical. Wind farms (WF) –that may consist of several hundred individual KW or MW wind turbines- arenormally located at the remote reaches of the power system. This wind power needs to be delivered to load centers throughlong-distance transmission lines. Most common generator technology used in wind turbines (WTs) was squirrel cage induction generators (SCIG) in the past. Despite some drawbacks, because of economic concerns these generators constitute a non-negligible share of currently installed wind energy capacity. Wind turbine generators (WTG) equipped with Doubly-Fed Induction Generator (DFIG) with advantages like wide wind speed range operation and reduced converter power are also widely employed in modern wind energy systems.

Connecting WFs to transmission networks encountered us with some newchallenges basically due to unpredictable and intermittent behavior of wind energy. Transmission lines protection in presence of these kinds of energy sources is one of these problems. When a disturbance occurs in power system, WF terminal would experience a voltage drop leading to a large current flowing through DFIG stator and as a consequence (due to the magnetic field interaction between stator and rotor) rotor circuit. This would hurt rotor circuit converter. WFs were formerly protected by simple under voltage relaying during power system faults. However as a result of the increased wind energy penetration, and in order to increase system stability, the new grid codes require WFs to remain connected to the power networks during disturbances. Conventionally Fault analysis and settings of protective relays have been founded upon this fact that power systems consist mainly of synchronous generators. Mean while, fault behavior of the newly integrated IGs is different from that of the SGs [1]. This difference can directly affect the performance of relays, particularly the ones that protect the lines connected to IG based WFs.

Distance relays are commonly used relays for line protection eitheras primary or backup. Ref. [1] is discussed about two types of WT generators apply most in WF, and proposed a current wave form based technique for impedance measuring of distance relays with quadratic characteristic. In [2] an adaptive setting is proposed for distance relays protecting lines connected to WFs. Ref. [3] also discusses an adaptive setting for distance relays with quadratic characteristic using neural networks without considering the type of WTs. Fault

Received November 5, 2015; Revised February 10, 2016; Accepted February 20, 2016

behavior and short circuit studies of WTs has alsoreceived a great deal of attention in relay settings. Ref. [4] studies different factors affecting short circuit current of WFs with various WT types. While in [5] short circuit current contribution of WTs is explored. Ref. [6] has particularly discussed short circuit current contribution of DFIG in comparison with induction machines.

The impact offault resistance and its location on transmission line voltage and current frequenciesconnected to DFIG-based WFs is not studied yet. Thus in the proposed paper, it will be demonstrated that different voltage and current fundamental frequencies will lead to inefficiency of conventional impedance measurements that are used in distance relays. Section 2 will briefly describe WTs with DFIG modeling. In section3 we will take a look at WF simplifications. Section 4 will describe DFIG short circuit behavior.Some analysis based on simulations done in PSCAD/EMTDC and investigations of impact of fault resistor and its location on fundamental frequency differences between voltage and current will be demonstrated in section 5. Finally conclusions will be presentedin section 6.

2. WT Generators with Doubly Fed Induction Generators Modeling

WT modeling generally consists of three parts. Aerodynamic, drive-train and induction generator modeling.

2.1. WT Aerodynamic modeling

The aerodynamic model of a WT can becharacterized by the well-known *CP-λ-β* curves [7]. An empirical relation described (equation **Error! Reference source not found.**) between *Cp* (rotor power coefficient), tip speed ratio (*λ*) and blade pitch angle (*β*) is used for developing a look-up table that provides a value of *Cp*for a given value of wind speed and tip speed ratio [8].

$$C_p(\lambda,\beta) = c_1\left(\frac{c_2}{\lambda_i} - c_3\beta - c_4\right)e^{-\frac{c_5}{\lambda_i}} + c_6\lambda \quad (1)$$

$$\frac{1}{\lambda_i} = \frac{1}{\lambda + 0.08\beta} - \frac{0.035}{\beta^3 + 1} \quad (2)$$

The coefficients c_1−c_6 are proposed as equal to: c_1 = 0.5, c_2 = 116, c_3 =0.4, c_4 = 0, c_5 = 5, c_6 = 21 [8] and λ is described in relation **Error! Reference source not found.** as:

$$\lambda = \frac{\omega_t \times R}{V_w} \quad (3)$$

Where *R* is the blade length in m, $\omega_t$is the WT rotational speed in rad/s, and $V_w$is the wind speed in m/s, andthe numerator (ω_t×R) represents the blade tip speed in m/s ofthe WT.

At a certain wind speed, there is aunique WT rotational speed to achieve the maximum power coefficient, C_{Pm}, and thereby the maximum mechanical (wind) power that is presented with equation **Error! Reference source not found.**:

$$P_m = \frac{1}{2}\rho.C_p.A_r.{V_w}^3 \quad (4)$$

Where ρ is the air density in kg/m^3, $A_r = \pi R^2$ is the area in m^{2}swept by the rotor blades [7].

2.2. Drive-Train Modeling

The low WTspeed is converted to a high speed in order to rotate DFIG rotor through a gearbox with shafts. The drive-train system will simply be modeledas a single lumped-mass system with the lumped inertiaconstant H_m, that is calculated by:

$$H_m = H_t + H_g \quad (5)$$

The electromechanical dynamic equation is then given by **Error! Reference source not found.**:

$$2H_m p\omega_m = T_m - T_e - D_m\omega_m \quad (6)$$

Where ω_m is the rotational speed of the lumped-mass system and $\omega_m = \omega_t = \omega_r$, D_m is the damping of the lumped system [7].

2.3. Induction Generator Modeling

The DFIG is an induction machine with a wound rotor where the rotor and stator are both connected to electrical sources, hence the term 'doubly-fed' Figure 1 [9]. The stator winding is directly connected to grid while rotor winding connection is through back to back converters.

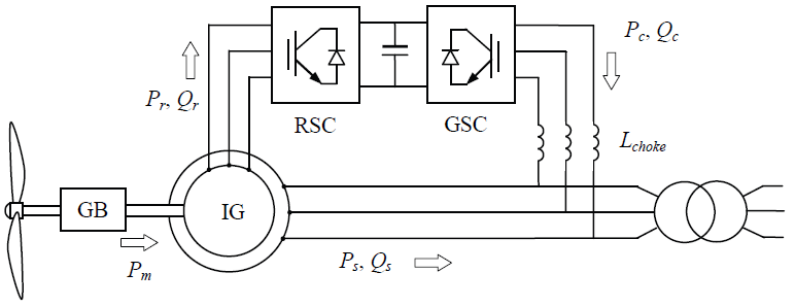

Figure 1. Doubly-fed induction generation system power flows [9].

Stator and rotor equations are described in matrix form at equations **Error! Reference source not found.** and **Error! Reference source not found.**.

$$\overline{V_{abcs}} = \overline{r_s \iota_{abcs}} + p\overline{\lambda_{abcs}} \quad (7)$$

$$\overline{V'_{abcr}} = \overline{r_r \iota'_{abcr}} + p\overline{\lambda'_{abcr}} \quad (8)$$

Where, λ is the flux linkage, subscripts s and r stand for variables and parameters associated with the stator and rotor side respectively. Equation **Error! Reference source not found.** represents machine parameters when referred to the rotor side. As it can be seen in relations **Error! Reference source not found.** and **Error! Reference source not found.** voltages, inductances and currentsare in the stationary *abc* reference frame. They are thus time-variant. Applying Park transform, the *abc* frame quantities are converted in qd0 frame quantities as in **Error! Reference source not found.** and **Error! Reference source not found.**. This frame is rotating at the synchronous frequency [8].

$$\overline{V_{qd0s}} = \overline{r_s \iota_{qd0s}} \pm \omega_s\overline{\lambda_{dqs}} + p\overline{\lambda_{qd0s}} \quad (9)$$

$$\overline{V'_{qd0r}} = \overline{r'_r \iota'_{qd0r}} \pm (\omega_s - \omega_r)\overline{\lambda'_{dqr}} + p\overline{\lambda'_{qd0r}} \quad (10)$$

ω_s and ω_r are the rotational speed of the synchronously rotating qd0 frame and rotor frame respectively.

It has been mentioned that the three phase rotor windings are connected to electrical source and are energized with three-phase currents. These rotor currents establish the rotor magnetic field. The rotor magnetic field interacts with the stator magnetic field to develop torque [9]. The per-unit electromagnetic torque equation is given by:

$$T_e = \lambda_{ds}i_{qs} - \lambda_{qs}i_{ds} = \lambda_{qr}i_{dr} - \lambda_{dr}i_{qr} = L_m\left(i_{qs}i_{dr} - i_{ds}i_{qr}\right) \quad (11)$$

The PSCAD/EMTDC software library provides the standard model of the wound rotor induction machine, whichis used in this study.

DFIG Converters Modeling

This section describes the modeling of a back-to-back converter system for a DFIG using field oriented control (FOC). The converters are modeled to be voltage source converters [8].

2.3.1. Grid-side Converter Control

The grid-side converter controls the flow of real and reactive power to the grid, through the grid interfacing inductances. The objective of the grid-side converter is to keep the dc-link voltage constant regardless of the magnitude and direction ofthe rotor power. The vector control method is used, with a reference frame oriented along the stator voltage vector position, enabling independent control of the active and reactive power flowing between the grid and the converter. The PWM converter is current regulated, with the d-axis current used to regulate the dc-link voltage and the q-axis current component to regulate the reactive power.

Figure *2* shows the schematic control structure of the grid-side converter.

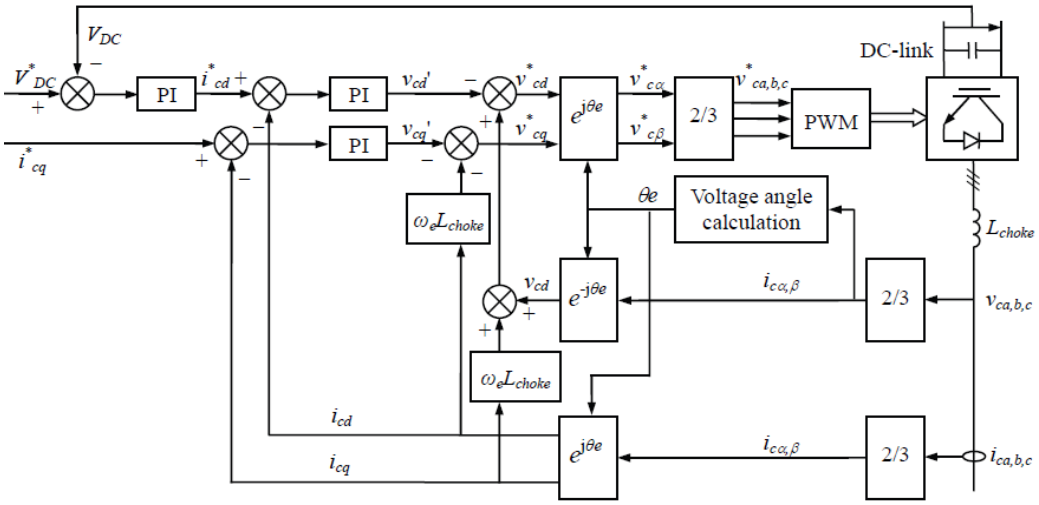

Figure 2. Grid side converter control

The voltage equations in synchronously rotating *dq*-axis reference frame are described by **Error! Reference source not found.** and **Error! Reference source not found.**:

$$v_{cd} = Ri_{cd} + L_{choke}\frac{di_{cd}}{dt} - \omega_e L_{choke} i_{cq} + v_{cd1} \quad (12)$$

$$v_{cq} = Ri_{cq} + L_{choke}\frac{di_{cq}}{dt} + \omega_e L_{choke} i_{cd} + v_{cq1} \quad (13)$$

Where v_{cd} and v_{cq} are d and q axis converter side voltages. R and L_{choke} are interface resistor and inductance with grid. The angular position of the grid voltage is calculated as

$$\theta_e = \int \omega_e dt = \tan^{-1}\left(\frac{v_{c\beta}}{v_{c\alpha}}\right) \quad (14)$$

Where $v_{c\alpha}$ and $v_{c\beta}$ are the converter grid-side voltage stationary frame components. The d-axis of the reference frame is aligned with the grid voltage angular position θ_e. Since the

amplitude of the grid voltage is constant, v_{cq} is zero and v_{cd} is constant. The active and reactive power will be proportional to i_{cd} and i_{cq} respectively. Assume the grid-side transformer connection is star, the converter active and reactive power flows described by equations **Error! Reference source not found.** and **Error! Reference source not found.**.

$$P_c = 3\left(v_{cd}i_{cd} + v_{cq}i_{cq}\right) = 3v_{cd}i_{cd} \quad (15)$$

$$Q_c = 3\left(v_{cd}i_{cq} + v_{cq}i_{cd}\right) = 3v_{cd}i_{cq} \quad (16)$$

Which demonstrates that the real and reactive powers from the grid-side converter are controlled by the i_{cd} and i_{cq} components of current respectively. To realize decoupled control, similar compensations are introduced likewise in equations **Error! Reference source not found.** and **Error! Reference source not found.**:

$$v^*_{cd} = -v'_{cd} + (\omega_e L_{choke} i_{cq} + v_d) \quad (17)$$

$$v^*_{cq} = -v'_{cq} - (\omega_e L_{choke} i_{cd}) \quad (18)$$

The reference voltagesv_{cd}^* and v_{cq}^* are then transformed by inverse-Park transformation to give3-phase voltage v_{cabc}^* for the final PWM signal generation for the converter IGBT switching.

2.3.2. Rotor-Side Converter Control

The rotor side converter (inverter) of the DFIG is connected to the grid side converter (rectifier) through a DC link capacitor. Actual active power is compared with the set-point value which is determined by the wind speed. A PI controller is used, as seen in

Figure *3*, to generate the required value of I_{dr}. Similarly, for the reactive power, a PI controller is used to generate the required I_{qr}. These values of I_{dr} and I_{qr} are transformed back into the *abc* frame to obtain the required value of rotor currents. Also seen in the

Figure *3*, is a hysteresis controller used to generate the switching sequence for the IGBT switches in the rotor side converter. Required rotor currents obtained in the *abc* frame are thus generated by using hysteresis control. A hysteresis band of 0.1% is used for the hysteresis controller.

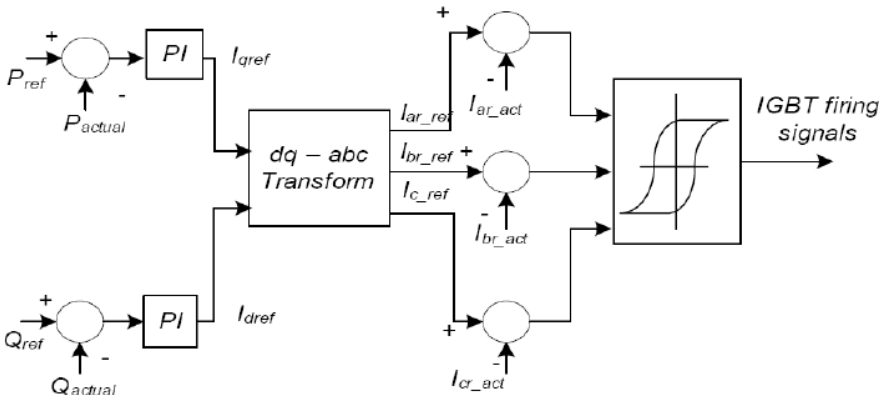

Figure 3. Rotor side converter control [8]

3. WF Simplification in Power System Studies

In order to WFs connection to grid for power system studies, there are some common simplifications. The common modeling method for doubly-fed WF dynamic equivalence can be divided into two kinds of representations: single-machine and multi-machine representation method.

3.1. Single-Machine Representation Method

Single-machine representation method refers to the whole WF is represented with one WT machine as the equivalent model. According to the difference of wind speed between all WTs, the method can be further classified into ‘’1+1’ model (namely one WT with one generator) and “n+1” model (namely n WTs with one generator). This classification is given in Figure 4.

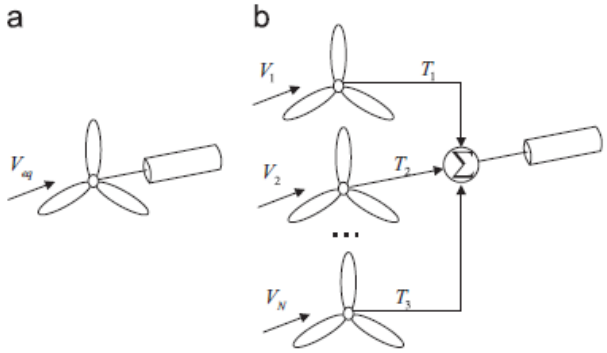

Figure 4. The classification of single machine representation method.
a. 1+1 representation. b. n+1 representation [10]

3.2. Multi-Machine Representation Method

Multi-machine representation method is aimed to build the “n+n” model (namelyn WT plus n generator) by introducing the idea of coherency-based equivalents, which is a common method for dynamic equivalence in the power system, to the dynamic equivalent modeling of the WF. The method is based on the principle of unit group that WTs have the same or similar operational point to combine the same group of units [10].

The employed simplification method of WFs here, is “1+1” representation method. Parameter equivalence is based on Table 1 Table *1*. DFIG equivalent model parameters[11].

Table 1. DFIG equivalent model parameters

Parameter	Equivalent DFIG
MVA	n × detailed DFIG10
V_{stator} (kV)	The same as detailed DFIG
p.u Parameters	The same as detailed DFIG

4. Short Circuit Behavior of DFIGs

Balanced fault current for a SCIG machine is consisted of a decaying dc and a decaying ac component, expressed by equation **Error! Reference source not found.**:

$$i_f(t) = \frac{V_{max}}{1-s}\left(\frac{1}{X'} - \frac{1}{X_{\sigma s} + 1.5X_{ms}}\right) e^{-t/T'} \times \cos\big((1-s)\omega_1 t + \theta\big) + \frac{V_{max}}{1-s}\left[\frac{1}{X'} e^{-t/Ta}\cos(\theta)\right] \quad (19)$$

Where V_{max} is the voltage amplitude, $\omega 1$ is the fundamental angular frequency, s is the IG slip, X' is the motor transient reactance, $X\sigma s$and X_{ms} are the leakage and magnetizing reactances of the stator winding, T' is the short-circuit transient time constant, which is inversely proportional to the rotor resistance, $T_a$is the stator time constant, and θ is the fault inception angle. Since the DFIGs protect with crowbar circuits, under severe fault conditions (like three phase balanced fault), crowbar circuit will be activated, rotor and stator converters will be short circuited and then the behavior of DFIGs conceptually is the same as SCIGs. Machine slip of the fault current in **Error! Reference source not found.** would affect quit different impact on short circuit current from distance relaying perspective [1]. DFIGs work under slip ranges of ±30%, commensurate with wind speed. Thus (1-s) factor here would not be a negligible term and in 60 Hz systems, causes a range of 42–78 Hz for DFIG fault currents. This means that fault current

frequency will generate off-nominal frequency that leads to impedance measuring (necessary for distance protection) problems.

5. Impact Analysis of Fault Resistor Size and its Location on Impedance Measuring

In this section power system presented in

Figure *5* is simulated in PSCAD and a symmetrical three phase-ground fault with changing resistor is applied on various locations of power system. Then fundamental frequencies of voltage and current of lines under fault and the line connected to WF are considered.

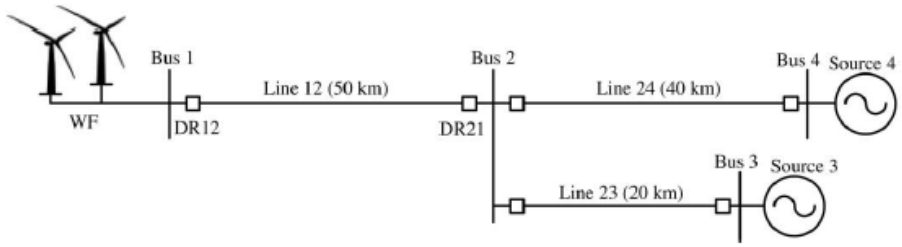

Figure 5. Single line diagram of the test power system [1]

A distance relay operates based on the fundamental frequency voltage and current phasors. For example, the phase A-ground element of a distance relay computes the impedance by relation **Error! Reference source not found.**:

$$Z_{ag} = \frac{V_{ag}}{I_a + kI_0} \quad (20)$$

Where V_{ag} and I_a are the fundamental frequency phasors for phase A voltage and current, k is the zero-sequence compensation factor, and I_o is the zero sequence current. Occurring a fault will result in frequency excursion conditions. In order to modify adaptively with these conditions and compute voltage and current phasors accurately, distance relays will be equipped with frequency tracking techniques. It will be demonstrated that in the case of DFIG based WFs during balanced faults, since the voltage frequency is dictated by the bulk power system, this frequency will remain within a narrow margin of 60 Hz. However current frequency significantly deviates from the nominal frequency. Thus relations such as **Error! Reference source not found.** is not hold true. To validate this difference between voltage and current frequency, balanced three phase faults with changing resistor size and location is applied to line 12 and line 24.

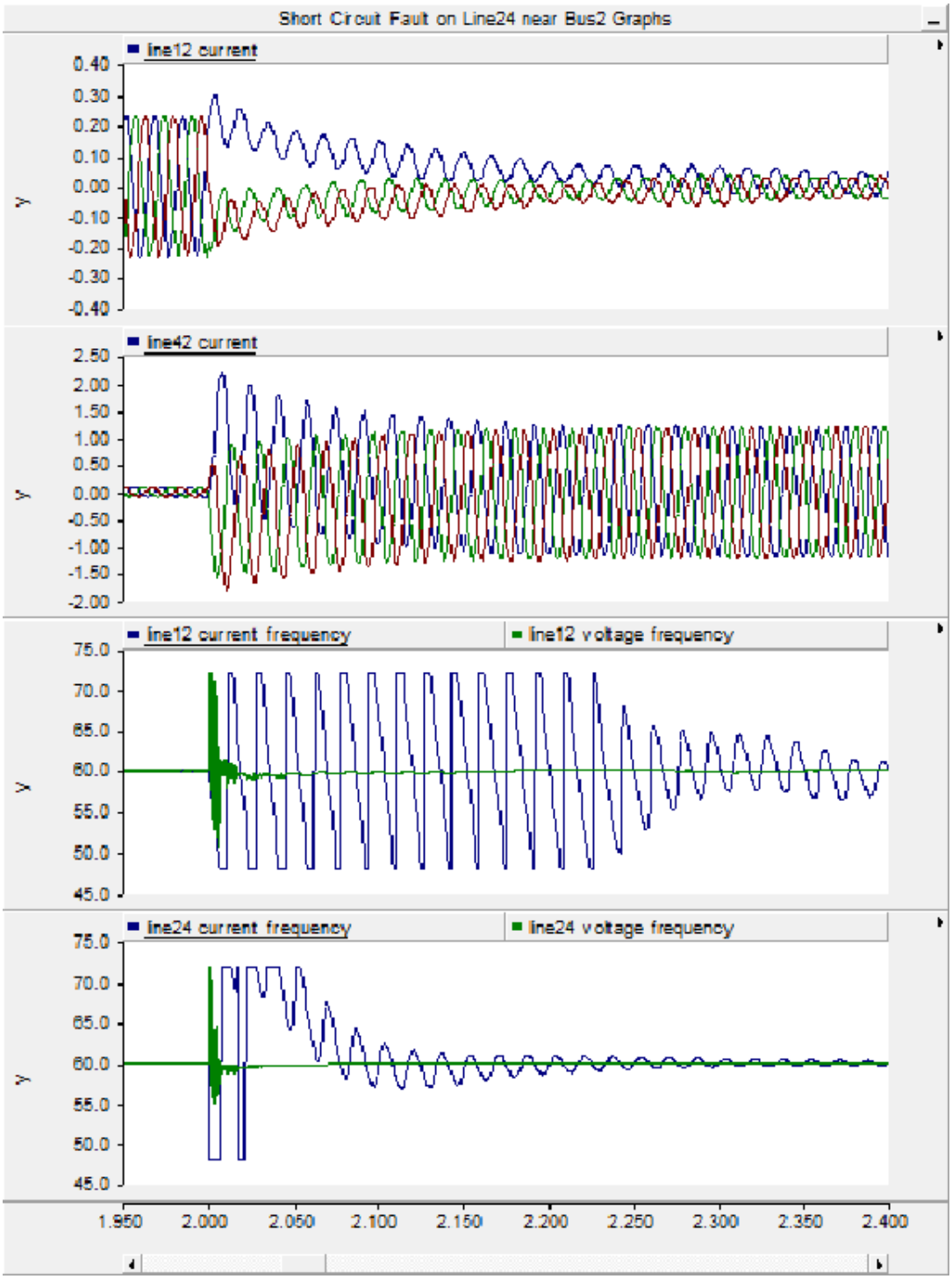

Figure 6. Short circuit fault at 50m of bus2 on line24 graphs

When a short circuit occurs near bus 2, because of the crowbar activation and also the non-negligible slip termin DFIG (equation **Error! Reference source not found.**), fault current in line connected to WF is damped fasterin comparison with the further line (line 24). Frequency fluctuations in line 24 is smaller than the line connected to WF. This would result in inaccurate impedance measuring in line 12 distance relay, leading to inefficiency of conventional distance relay impedance measuring algorithms.

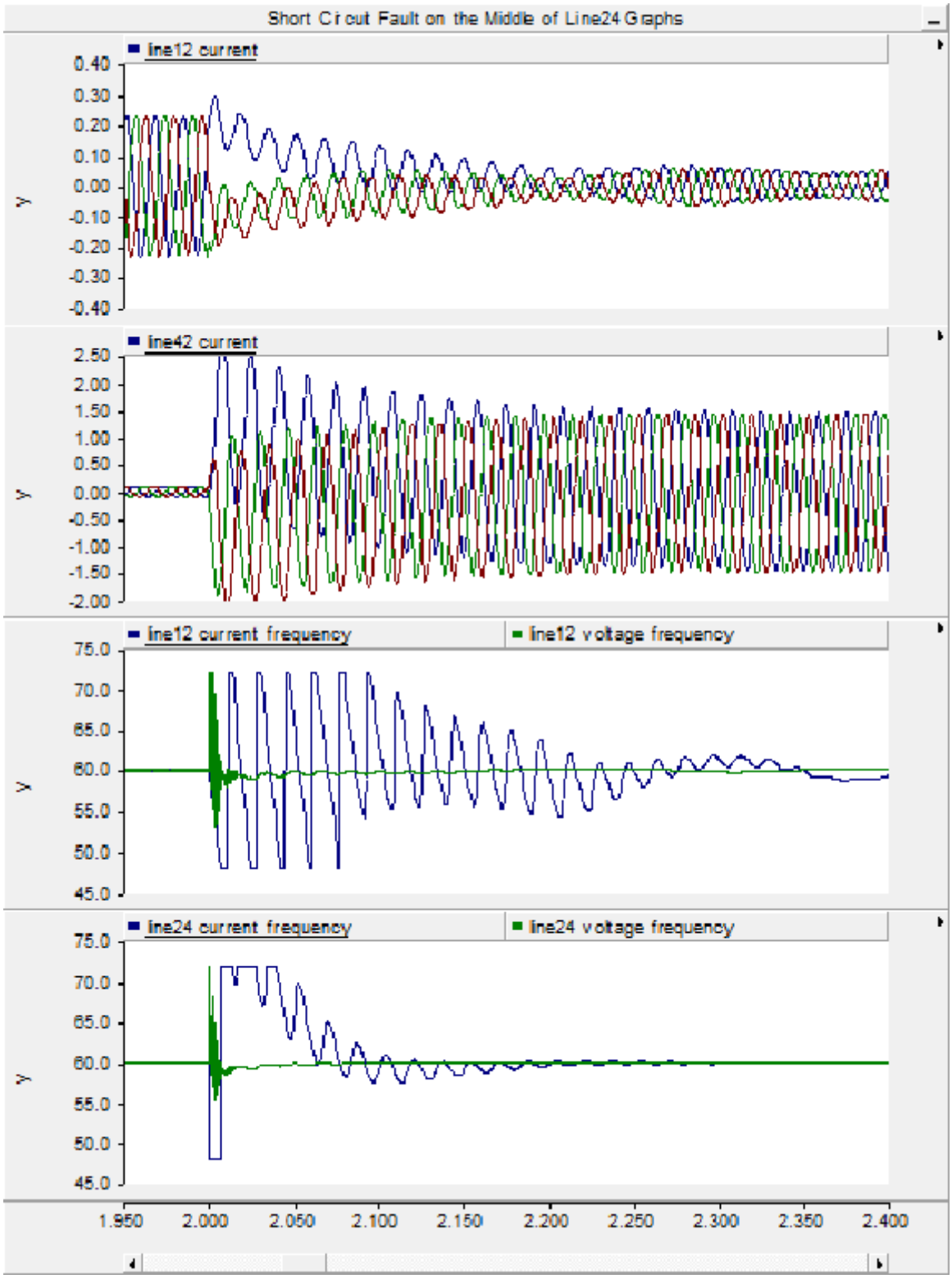

Figure 7. Short circuit fault on the middle of lin 24 graphs

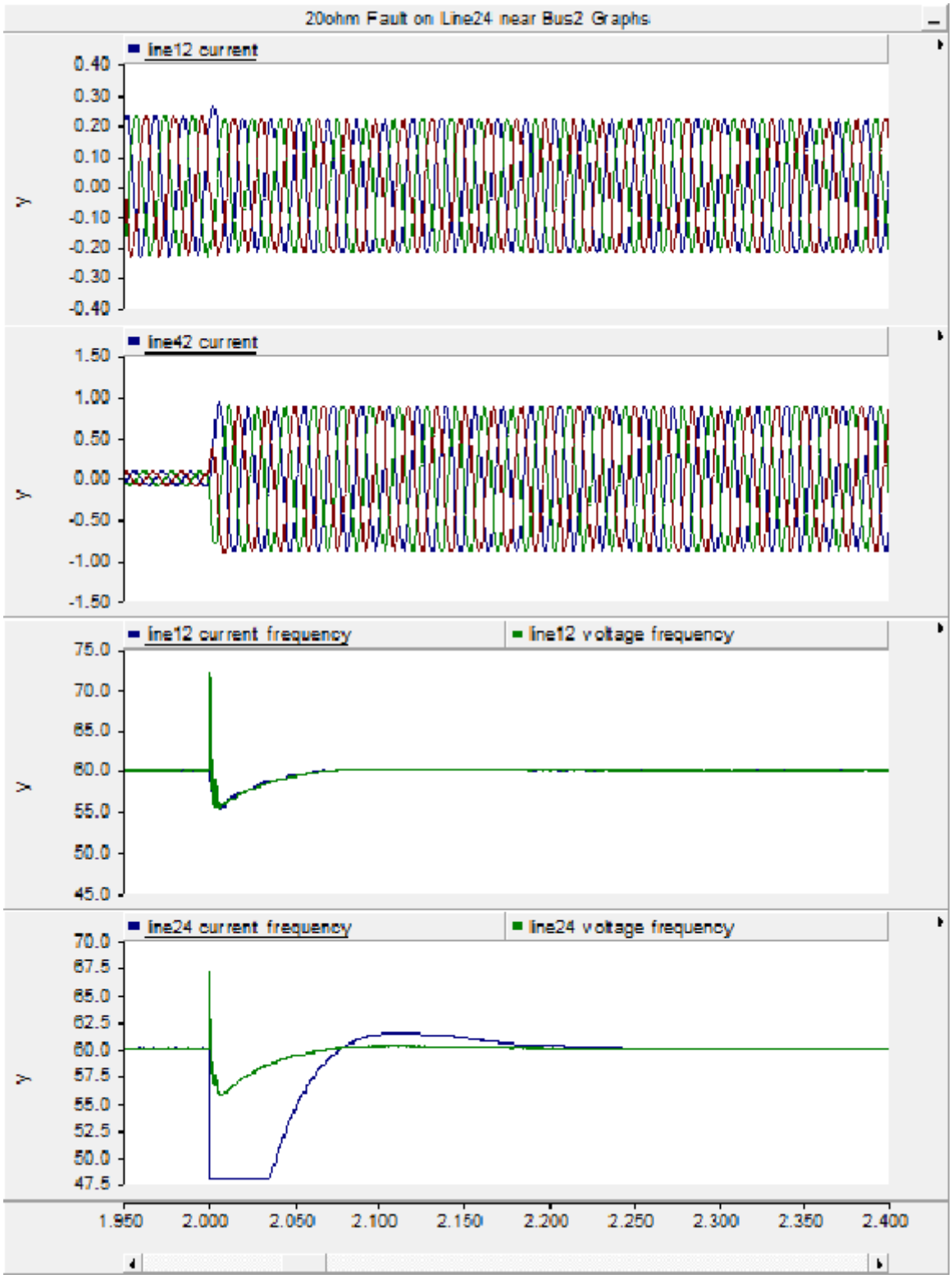

Figure 8. R_f = 20 ohm at 50 m of bus 2 on line 24

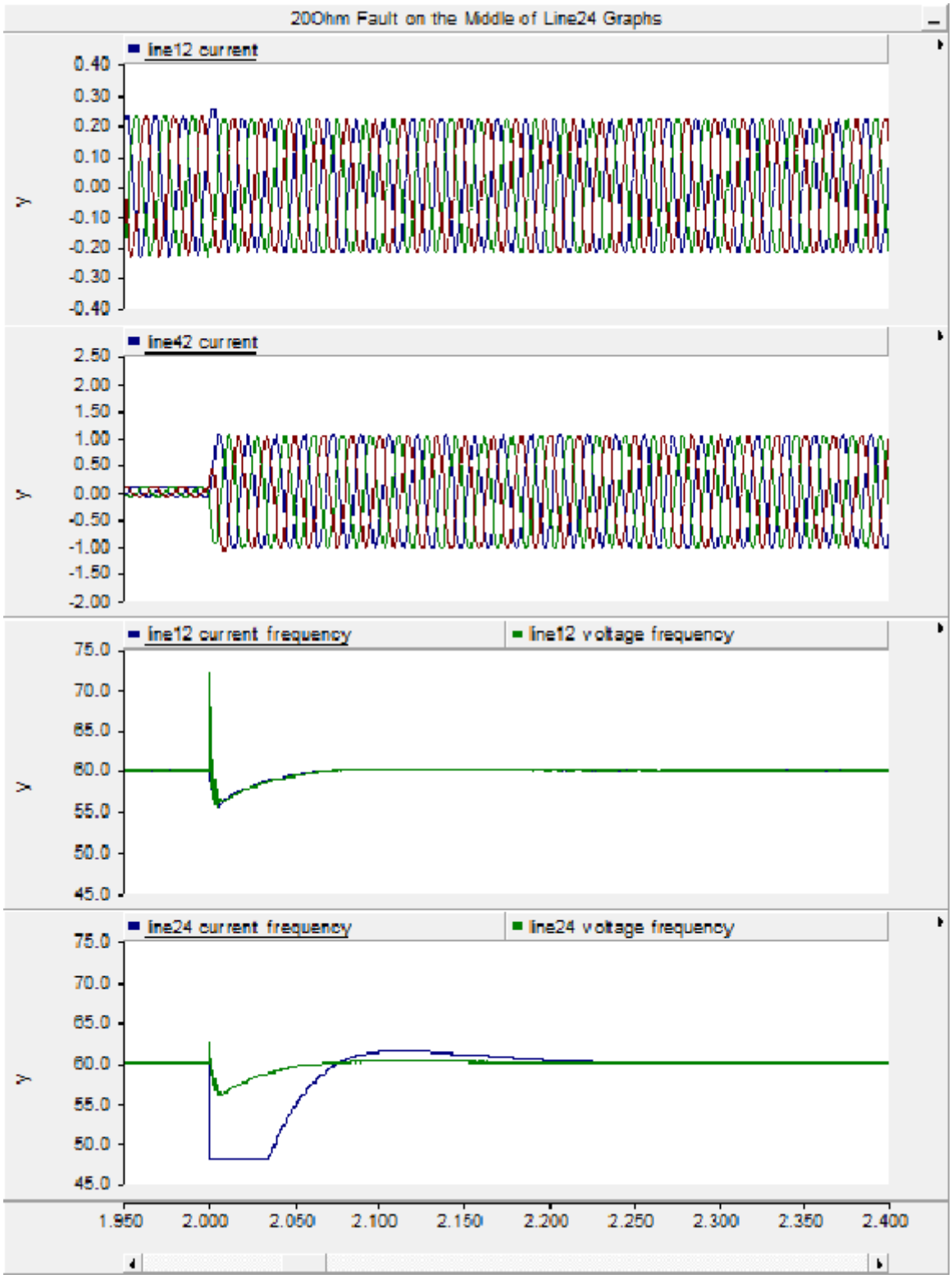

Figure 9. R_f = 20 ohm fault on the middle of line 24

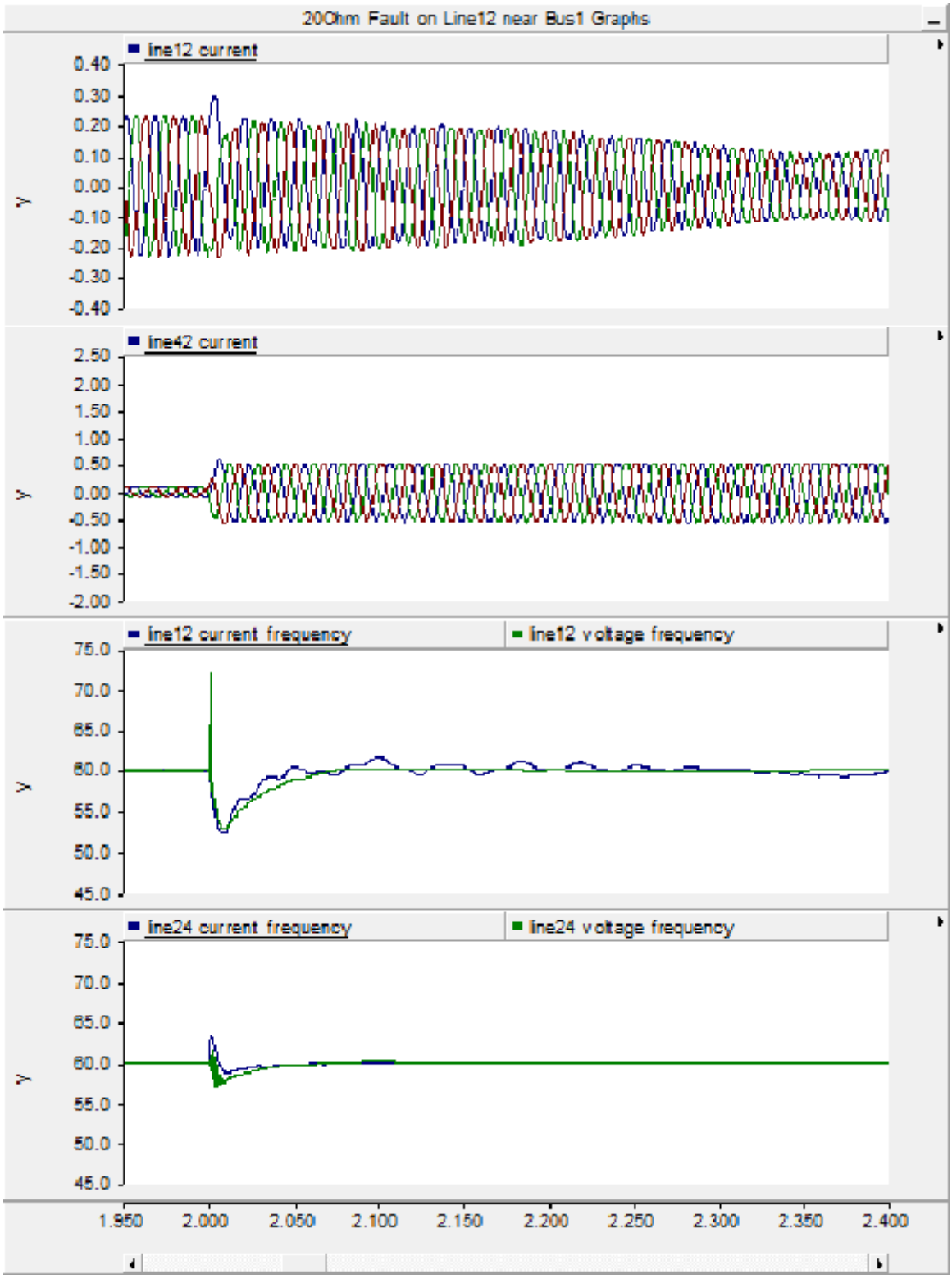

Figure 10. R_f = 20 ohm on 50 m of bus1 on line 12

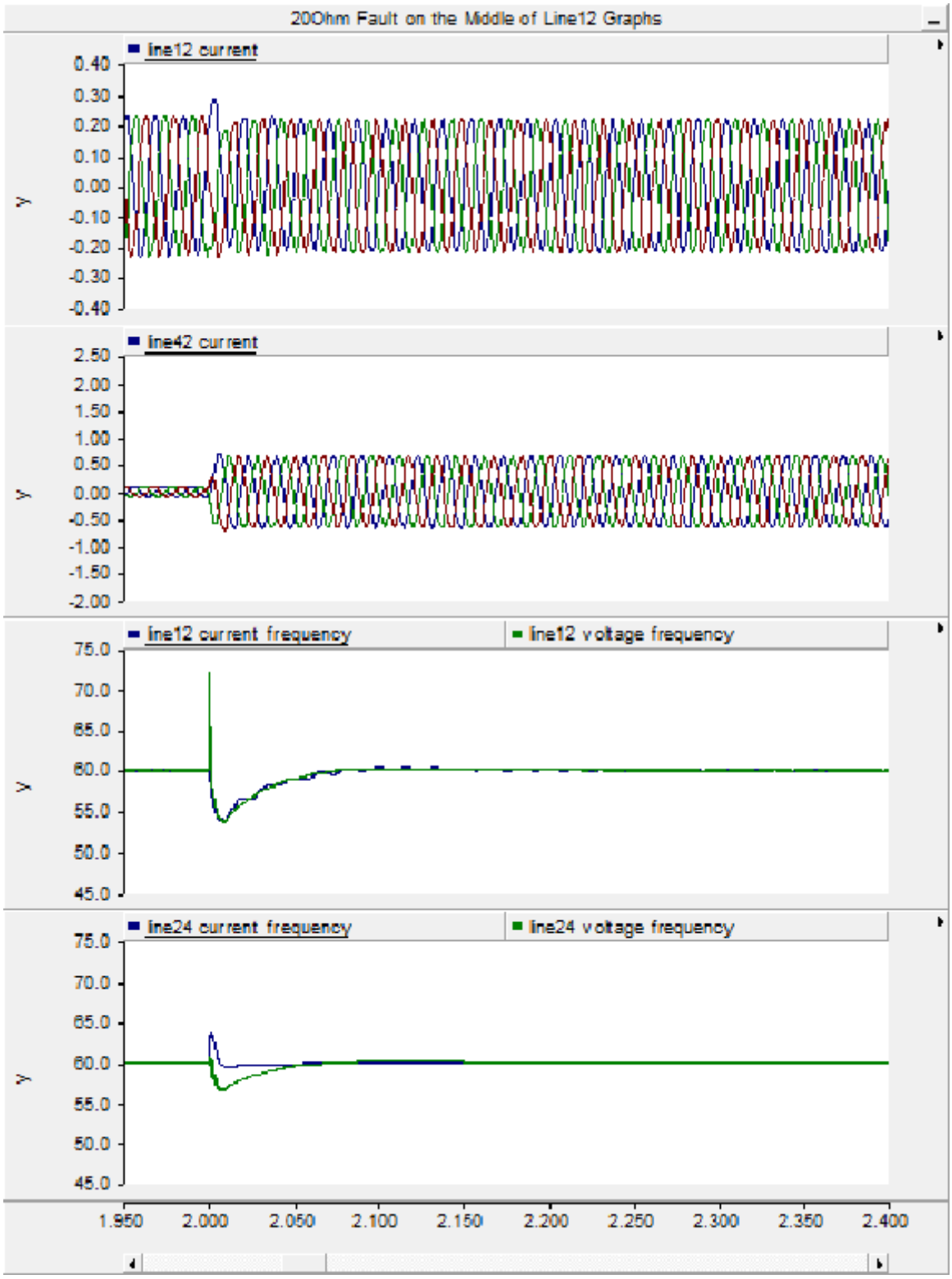

Figure 11. R_f = 20 ohm on the middle of line 12

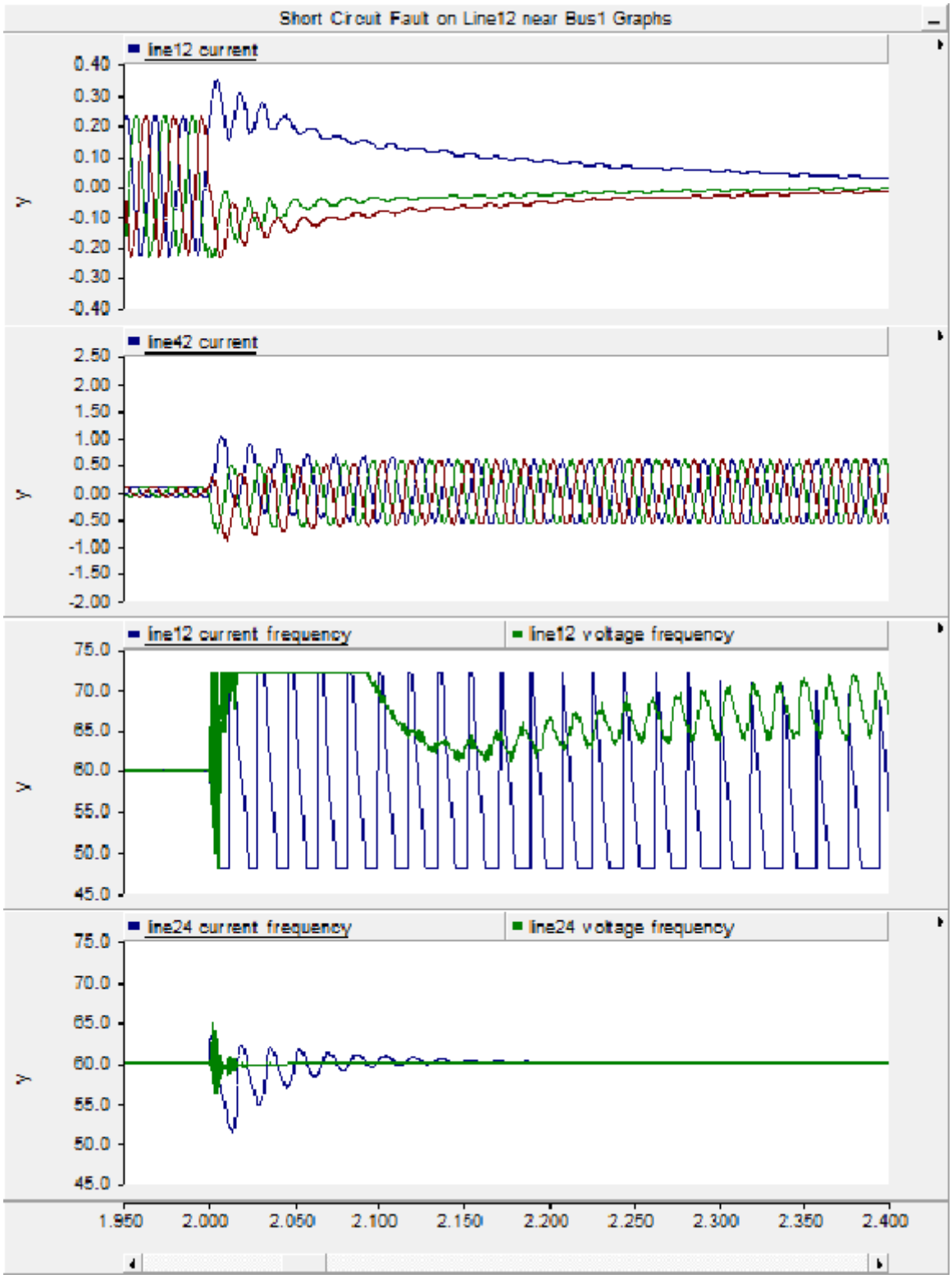

Figure 12. Short circuit fault on line 12 50 m of bus1

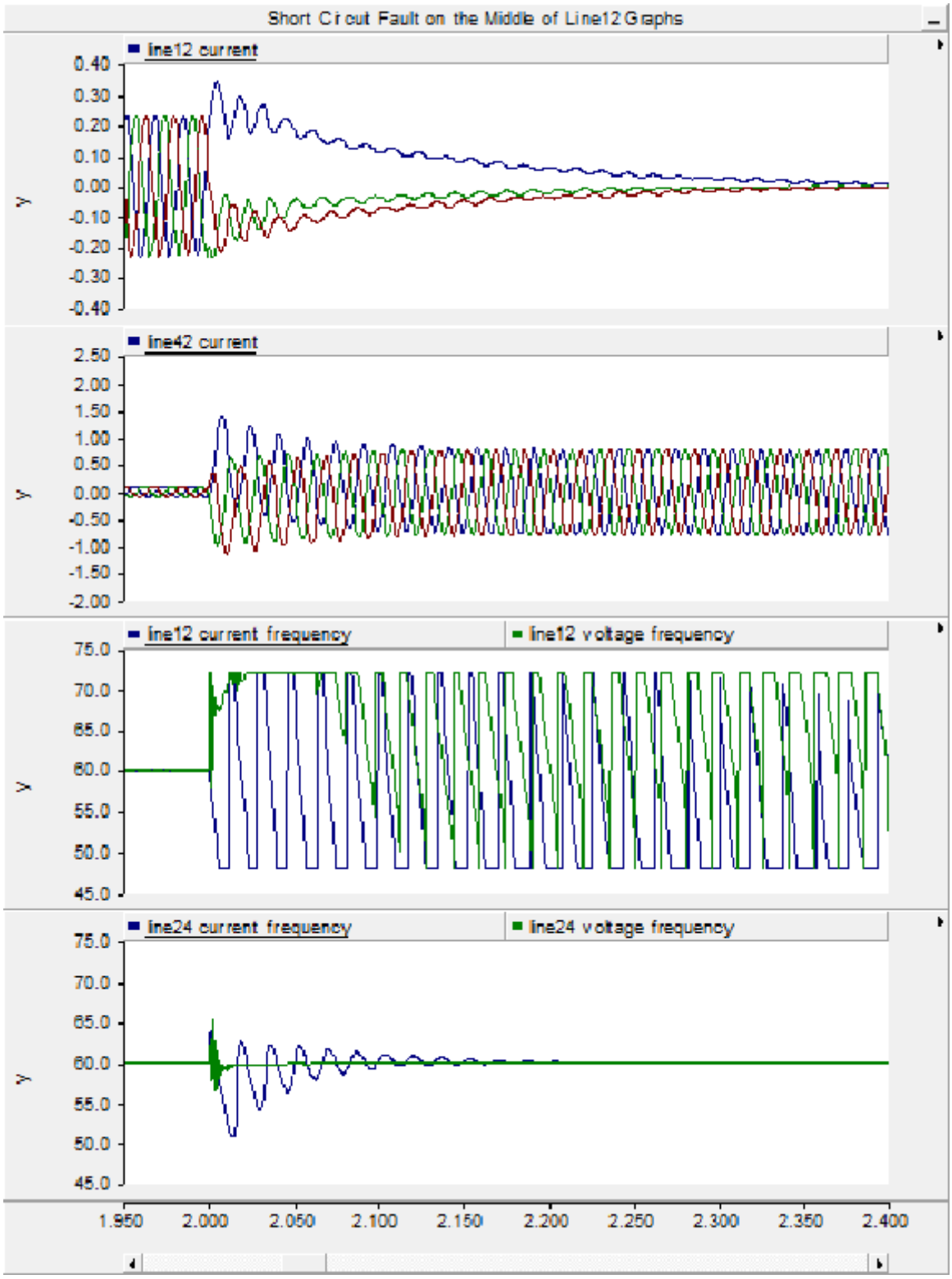

Figure 13. Short circuit fault on middle of line 12

As it is can be seen from above simulations, the difference between voltage and current frequencies under balanced short-circuits, results to a new and unfamiliar situation from the protective relaying perspective. Since equation **Error! Reference source not found.** and such

impedance measurement equations are founded upon phasor quantities corresponding to the same frequency, these relations do not hold true anymore. However for the faults with larger resistors, since the voltage and current frequencies have no distinctive differences, the conventional methods are still true. The test power system connected to DFIG based WF details is described in [1].

6. Conclusion

When a fault occurs ona transmission line connected to DFIG based WF with fault ride through capability, the smaller the fault resistor, the more severe current frequency excursions. If the fault is close to WF, voltage frequency fluctuations on transmission line connected to WFare distinctive. Theoff-nominal frequency of a DFIG based WF fault current would have a high impact on distance protection performance. Thereforenew methods and approaches are requiredin impedance measuringfor distance relays.

References

[1] A Hooshyar, MA Azzouz, and EF El-Saadany. "Distance Protection of Lines Connected to Induction Generator-Based Wind Farms During Balanced Faults". *IEEE Transactions on Sustainable Energy*. 2014; 5: 1193-1203.
[2] A Pradhan and G Joos. "Adaptive distance relay setting for lines connecting wind farms". *IEEE Transactions on Energy Conversion*. 2007; 22: 206-213.
[3] H Sadeghi. "A novel method for adaptive distance protection of transmission line connected to wind farms". *International Journal of Electrical Power & Energy Systems.* 2012; 43: 1376-1382.
[4] E Muljadi, N Samaan, V Gevorgian, J Li, and S Pasupulati. "Different factors affecting short circuit behavior of a wind power plant". *IEEE Transactions on Industry Applications*. 2013; 49: 284-292.
[5] E Muljadi, N Samaan, V Gevorgian, J Li, and S Pasupulati. "Short circuit current contribution for different wind turbine generator types". in *Power and Energy Society General Meeting, 2010 IEEE*. 2010: 1-8.
[6] J Morren and SW De Haan. "Short-circuit current of wind turbines with doubly fed induction generator". *IEEE Transactions on Energy Conversion*. 2007; 22: 174-180.
[7] W Qiao. "Dynamic modeling and control of doubly fed induction generators driven by wind turbines". in *Power Systems Conference and Exposition, 2009. PSCE'09. IEEE/PES*. 2009, pp. 1-8.
[8] MG Vyas. "Simulation and modeling of wind power plants: a pedagogical approach". 2010.
[9] J Fletcher and J Yang. *Introduction to the Doubly-Fed Induction Generator for Wind Power Applications*. INTECH Open Access Publisher. 2010.
[10] J Zou, C Peng, Y Yan, H Zheng, and Y Li. "A survey of dynamic equivalent modeling for wind farm". *Renewable and Sustainable Energy Reviews*. 2014; 40: 956-963.
[11] T Wang, E Makram, R Hadidi, and X Xu. "The Impact of the Offshore Wind Farm Switching Transient Operation on Power System". *Journal of Power and Energy Engineering*. 2014; 2014.